Mutual regulation of CD4+ T cells and intravascular fibrin in infections

Tonina T. Mueller,[1,2*] Mona Pilartz,[1*] Manovriti Thakur,[1*] Torben LangHeinrich,[1] Junfu Luo,[1] Rebecca Block,[1] Jonathan K.L. Hoeflinger,[1] Sarah Meister,[1] Flavio Karaj,[1] Laura Garcia Perez,[3] Rupert Öllinger,[4] Thomas Engleitner,[4] Jakob Thoss,[1] Michael Voelkl,[1] Claudia Tersteeg,[5] Uwe Koedel,[6] Alexander Zigman Kohlmaier,[1] Daniel Teupser,[1] Malgorzata Wygrecka,[7] Haifeng Ye,[8] Klaus T. Preissner,[9] Helena Radbruch,[10] Sefer Elezkurtaj,[11] Matthias Mack,[12] Philipp von Hundelshausen,[13] Christian Weber,[13] Steffen Massberg,[2] Christian Schulz,[2] Roland Rad,[4] Samuel Huber,[3] Hellen Ishikawa-Ankerhold[2#] and Bernd Engelmann[1#]

[1]Institut für Laboratoriumsmedizin, Klinikum der Universität München, Ludwig-Maximilians-Universität (LMU), Munich, Germany; [2]Medizinische Klinik I, Klinikum der Universität München, LMU, Munich, Germany; [3]1. Medizinische Klinik und Poliklinik, Universitätsklinikum Hamburg-Eppendorf, Hamburg, Germany; [4]Institut für Molekulare Onkologie und Funktionelle Genomik, Technische Universität München, Munich, Germany; [5]Laboratory for Thrombosis Research, KU Leuven Campus Kulak Kortrijk, Kortijik, Belgium; [6]Neurologische Klinik, Klinikum der Universität München, LMU, Munich, Germany; [7]Center for Infection and Genomics of the Lung (CIGL), Justus-Liebig-Universität, Giessen, Germany; [8]Institute of Regenerative Biology and Medicine, Helmholtz-Zentrum München, Munich, Germany; [9]Institute of Biochemistry, Justus-Liebig-Universität, Giessen, Germany; [10]Institut für Neuropathologie, Charité - Universitätsmedizin, Berlin, Germany; [11]Institut für Pathologie, Charité - Universitätsmedizin, Berlin, Germany; [12]Medizinische Klinik II, University of Regensburg, Regensburg, Germany and [13]Institut für Prophylaxe und Epidemiologie der Kreislaufkrankheiten, Ludwig-Maximilians-Universität, Munich, Germany

*TTM, MP and MT contributed equally as first authors.

#HI-A and BE contributed equally as senior authors.

Correspondence: B. Engelmann
Bernd.Engelmann@med.uni-muenchen.de

T.T. Mueller
Tonina.Mueller@med.uni-muenchen.de

Received: November 5, 2023.
Accepted: March 25, 2024.
Early view: April 4, 2024.

https://doi.org/10.3324/haematol.2023.284619

Abstract

Innate myeloid cells especially neutrophils and their extracellular traps are known to promote intravascular coagulation and thrombosis formation in infections and various other conditions. Innate myeloid cell-dependent fibrin formation can support systemic immunity while its dysregulation enhances the severity of infectious diseases. Less is known about the immune mechanisms preventing dysregulation of fibrin homeostasis in infection. During experimental systemic infections local fibrin deposits in the liver microcirculation cause rapid arrest of CD4+ T cells. Arrested T-helper cells mostly represent Th17 cells that partially originate from the small intestine. Intravascular fibrin deposits activate mouse and human CD4+ T cells which can be mediated by direct fibrin-CD4+ T-cell interactions. Activated CD4+ T cells suppress fibrin deposition and microvascular thrombosis by directly counteracting coagulation activation by neutrophils and classical monocytes. T-cell activation, which is initially triggered by IL-12p40- and MHC-II-dependent mechanisms, enhances intravascular fibrinolysis via LFA-1. Moreover, CD4+ T cells disfavor the association of the thrombin-activatable fibrinolysis inhibitor (TAFI) with fibrin whereby fibrin deposition is increased by TAFI in the absence but not in the presence of T cells. In human infections thrombosis development is inversely related to microvascular levels of CD4+ T cells. Thus, fibrin promotes LFA-1-dependent T-helper cell activation in infections which drives a negative feedback cycle that rapidly restricts intravascular fibrin and thrombosis development.

Introduction

Inflammation and thrombosis are closely coupled responses to infections.[1] Innate immune cells such as neutrophils and monocytes are quintessential activators of fibrin formation and mediators of thrombosis during systemic immune processes. Through expulsion of neutrophil extracellular traps (NET) neutrophils promote thrombosis

via different mechanisms that help to initiate and stabilize developing thrombi.[2] Monocytes trigger fibrin formation by activating the NLRP3 inflammasome and subsequent release of tissue factor (TF) through pyroptosis.[3]

During systemic infections activation of intravascular coagulation promotes the formation of microvascular thrombi that can restrict the dissemination and survival of bacteria.[4] Innate immune cell-controlled coagulation activation inside the microvasculature can thus participate in antimicrobial defense, analogous to the protective function of coagulum formation in evolutionarily ancient organisms.[5] So far, it is only incompletely known whether immune cells apart from innate leukocytes, especially cells of the lymphocyte lineage, participate in controlling intravascular coagulation and microvascular thrombosis during infections.

Aberrant fibrin generation and dysregulated micro- and macrovascular thrombosis can be detrimental consequences of innate immune responses to severe infections. Pathological thrombosis in connection with inflammation critically aggravates the morbidity and mortality of SARS-CoV-2 infections[6] and sepsis.[7] Hence, it is of particular interest to dissect the endogenous mechanisms that restrict intravascular fibrin generation in infection. Endothelial cells are known to be critical protectors against excessive fibrin deposition in the microcirculation such as via production of anticoagulant molecules including activated protein C and local stimulation of fibrinolysis.

Here we identify close bidirectional connections between $CD4^+$ T cells and microvascular fibrin homeostasis in vascular infection. Local fibrin deposits are shown to promote the arrest and LFA-1-dependent activation of $CD4^+$ T cells in the microcirculation. Activated T-helper cells rapidly restrict innate myeloid-cell driven thrombosis at and, favored by T-cell migration, distant from their arrest sites by stimulating fibrinolysis and disabling fibrinolysis inhibition.

Methods

Mice

Male and female WT, $plg^{-/-}$ and $f12^{-/-}$ mice (10-14 weeks old, age-matched) were infected with *E. coli* (3.2×10^8) or S. *pneumoniae* (1×10^8) via tail vein injection. Rivaroxaban (Santa Cruz) was injected at 3 mg/kg body weight 4 hours (h) before infection. Cell depletion and neutralization was performed as described in the *Online Supplementary Appendix*. All animal experiments were approved by the local authorities (Regierung von Oberbayern).

Kaede experiments

The small intestine of *kaede* x *Il17a*^{Katushka} mice was surgically exposed to photoconvert the accessible cells (dorsal and ventral) with BlueWave LED Prime UVA (Dymax) for two-times 30 seconds. Twenty-four h later mice were infected with *E. coli*.[8] Flow cytometry was performed as described in the *Online Supplementary Appendix*.

Isolation and migration of $CD4^+$ T cells

For intravital imaging or adoptive transfer experiments mouse $CD4^+$ T cells were isolated from spleen of uninfected C57BL/6J donor mice. Blood was collected from healthy human donors as approved by the local ethics committee of the Medical Faculty of LMU Munich. Human $CD4^+$ T cells were isolated from peripheral blood according to the manufacturer´s instructions ($CD4^+$ T Cell Isolation Kit, 130-096-533, Miltenyi Biotec). Cells were incubated on fibrin or poly-L-ornithine-coated microscopic glass slides with α-human CD3 antibody (5 μg/mL, HIT3a, Biolegend) and α-human CD28 antibody (5 μg/mL, CD28.2, Biolegend) or treated with either an immunoglobulin G (IgG) control or an anti-human LFA-1 antibody (20 μg/mL, BioXCell). Isolated $CD4^+$ T cells were fixed, blocked and incubated with AF647-labeled αCD69 antibody (1 μg/mL, Biolegend) and Dapi (1 μg/mL, Sigma Aldrich). For each experiment at least ten visual fields (225x225 μm) per donor were analyzed by confocal microscopy.

Immunohistochemistry

Murine livers and lungs were collected and fixed with neutral buffered 4% paraformaldehyde (PFA) at 4˚C for 1 h, dehydrated in 30% sucrose for 24 h at 4˚C and embedded in Tissue Tek; 10 μm cryosections were fixed in 4% PFA, washed and blocked with 2% bovine serum albumin solution or with 10% goat serum (Sigma Aldrich). For permeabilization, 0.1-0.3% Triton-X 100 was added. Tissue sections were incubated with unlabeled or labeled primary antibodies for 1 h at room temperature or overnight at 4°C. The labeling of primary antibodies was performed according to the manufacturer´s instructions (A20181, Thermo Fisher Scientific).

Tissue samples from the lung of patients with acute respiratory distress syndrome caused by infections with SARS-CoV-2 (N=12) or influenza virus (N=8) were obtained from autopsies. SARS-CoV-2 or influenza infections were diagnosed by PCR *ante mortem*. Mean age was 78.7±2.6 (SARS-CoV-2) and 68.1±5.5 years (influenza); 41.7% (SARS-CoV-2) and 37.5% (influenza) of the patients were female, respectively (*Online Supplementary Figure S6A*).

Plasmin formation by mouse and human T-helper cells

In order to analyze the fibrinolytic activity of different immune cells, plasmin formation was determined. For clot preparation, plasminogen (1 mg/mL, Sigma Aldrich) and fibrinogen (2.5 mg/mL, Sigma Aldrich) (1:80 volume/volume [vol/vol]) were mixed and thrombin was added (4 U/ml; 3:1 vol/vol, Sigma Aldrich). The suspension was incubated for 1 h at 37°C in 96-well plates. Afterwards chromogenic substrate S-2251 (1.5 mmol/L, Diapharma) and T-helper cells

(mouse: 100,000 cells/well, human: 100,000 cells/well) were added. In the case of human T-helper cells, T cells were activated on fibrin-coated 96 well plates in the presence of αCD3 and αCD28 antibodies as described above, and plasmin formation registered *in situ*. The optical density (A_{405}) was determined every 5 to 10 minutes to measure the protease activity of the generated plasmin.

RNA sequencing

$CD4^+$ T cells were isolated from the liver of uninfected and infected wild-type (WT) mice as described above. Library preparation for bulk-sequencing of poly(A)-RNA was done largely as described previously.[9]

Results

$CD4^+$ T cells restrict intravascular fibrin deposition in early systemic infections

In order to identify the immune cells regulating intravascular coagulation during systemic infections with *E. coli* we imaged nucleated cells arrested in the liver microcirculation, the major site of bacterial colonization. Neutrophils ($Ly6G^+$), classical ($Ly6C^+Ly6G^-$) and non-classical monocytes ($CX3CR1^+Ly6C^-$), $CD4^+$ T cells and B cells ($CD19^+$) were recruited to the liver microcirculation with different kinetics (Figure 1A). T-helper cells represented largely Th17 cells ($ROR\gamma T^+$) and regulatory T cells ($Foxp3^+$; Treg) and lower amounts of Th2 cells, while B cells were mostly B1a cells ($CD5^+$) (Figure 1A; *Online Supplementary Figure 1A*).

Since the role of T-helper cells in systemic infections and coagulation is incompletely defined and T-helper cells were recruited as abundantly as myeloid cells we analyzed their transcriptomic profiles. Unbiased analyses of the mRNA expressions of liver-resident $CD4^+$ T cells indicated the enrichment of genes predicted to be involved in innate immune responses (Figure 1B; confirming pro-inflammatory functions of T-helper cells[10]). Remarkably, the gene cluster with the second highest enrichment score represented T-cell genes implicated in blood coagulation. Among the coagulation genes regulators of fibrinolysis predominated during early infection (Figure 2A).

Microvascular fibrin deposition was highest 3 h after infection (*Online Supplementary Figure S1B*). Analyses of fibrin formation in systemic blood at the same time point indicated no change in coagulation time or other parameters compared to non-infected controls (*Online Supplementary Figure S1C*). tPA levels in systemic blood were increased by infection consistent with increased fibrinolysis (*Online Supplementary Figure S1D*). Imaging of coagulation proteins in the microcirculation showed that basic mediators of fibrinolysis (plasminogen, tPA, uPA, uPAR) were associated with $CD4^+$ T cells at the peak of fibrin formation (Figure 2B). TF, the initiator protein of coagulation, was mostly associated with classical monocytes and neutrophils (Figure 2B[11-13]). Overall, $CD4^+$ T cells represented the immune cell with the highest association of fibrinolysis activators (Figure 2B). Comparisons between different T-helper cell subtypes indicated that most of the Th17 cells and part of the Treg and Th2 cells were positive for the plasminogen activator uPA (*Online Supplementary Figure S1E*).

Next, we investigated whether T-helper cell-regulated fibrin deposition. Depletion of T-helper cells strongly reduced circulating $CD4^+$ T cells (*Online Supplementary Figure S1F*). Moreover, arrest of $CD4^+$ T cells in the liver microcirculation was completely abolished by depletion of $CD4^+$ T cells (from 5.2 to 0.07 $CD4^+$ T cells/visual field). $CD4^+$ T-cell depletion sharply increased fibrin deposition in microvessels of the liver and the lung (Figure 3A, B). Particularly, the absence of $CD4^+$ T-cell enhanced microvascular thrombosis (Figure 3A). Also, fibrin deposition and thrombus formation occasionally observed in larger vessels were increased after $CD4^+$ T-cell depletion (Figure 3C). Aspartate aminotransferase and alanine aminotransferase, indicators of liver tissue damage, were largely unchanged in early infection both in the presence and absence of T cells (*Online Supplementary Figure S1G*). Thus $CD4^+$ T cells inhibited fibrin deposition and development of thrombosis during systemic infection.

In contrast to the changes by T-helper loss, depletion of neutrophils (which reduced circulating neutrophils by 93%) decreased fibrin deposition (*Online Supplementary Figure S2A*). Moreover, intravascular fibrin was reduced in the absence of classical monocytes (*Online Supplementary Figure S2A*). Thus $CD4^+$ T cells rapidly suppress fibrin deposition during initial fibrin formation and thereby counteract procoagulant neutrophils and classical monocyte. In advanced stages of venous thrombosis and under non-infectious conditions, neutrophils and $CD4^+$ T cells especially Treg[14] cooperatively enhance resolution of venous thrombosis.[15] Depletion of Treg only slightly increased fibrin deposition in early systemic infection (*Online Supplementary Figure S2B*). This suggested that other T-cell subtypes such as Th17 cells contributed predominantly to restrict fibrin deposition and indicated that under infectious conditions $CD4^+$ T cells acted as direct antagonists of innate myeloid cells. Similar to *E. coli* infection, infection with the Gram-positive *S. pneumoniae* triggered microvascular fibrin generation in the liver and the lung (Figure 3D). $CD4^+$ T-cell depletion also amplified fibrin deposition in streptococcal infection (Figure 3D).

$CD4^+$ T cells stimulate fibrinolysis in early infection

In order to dissect the activity of T-cell-associated fibrinolysis activators $CD4^+$ T cells were isolated from uninfected and infected mice and analyzed for their ability to support formation of plasmin *ex vivo*. T cells from infected mice and, less so, from uninfected mice, promoted plasmin formation (Figure 4A). Moreover, isolated human T-helper cells supported plasmin formation which was enhanced by T-cell receptor (TCR)-dependent T-cell activation (*Online Supplementary Figure S2C*[16]). Next, activated mouse $CD4^+$ T cells

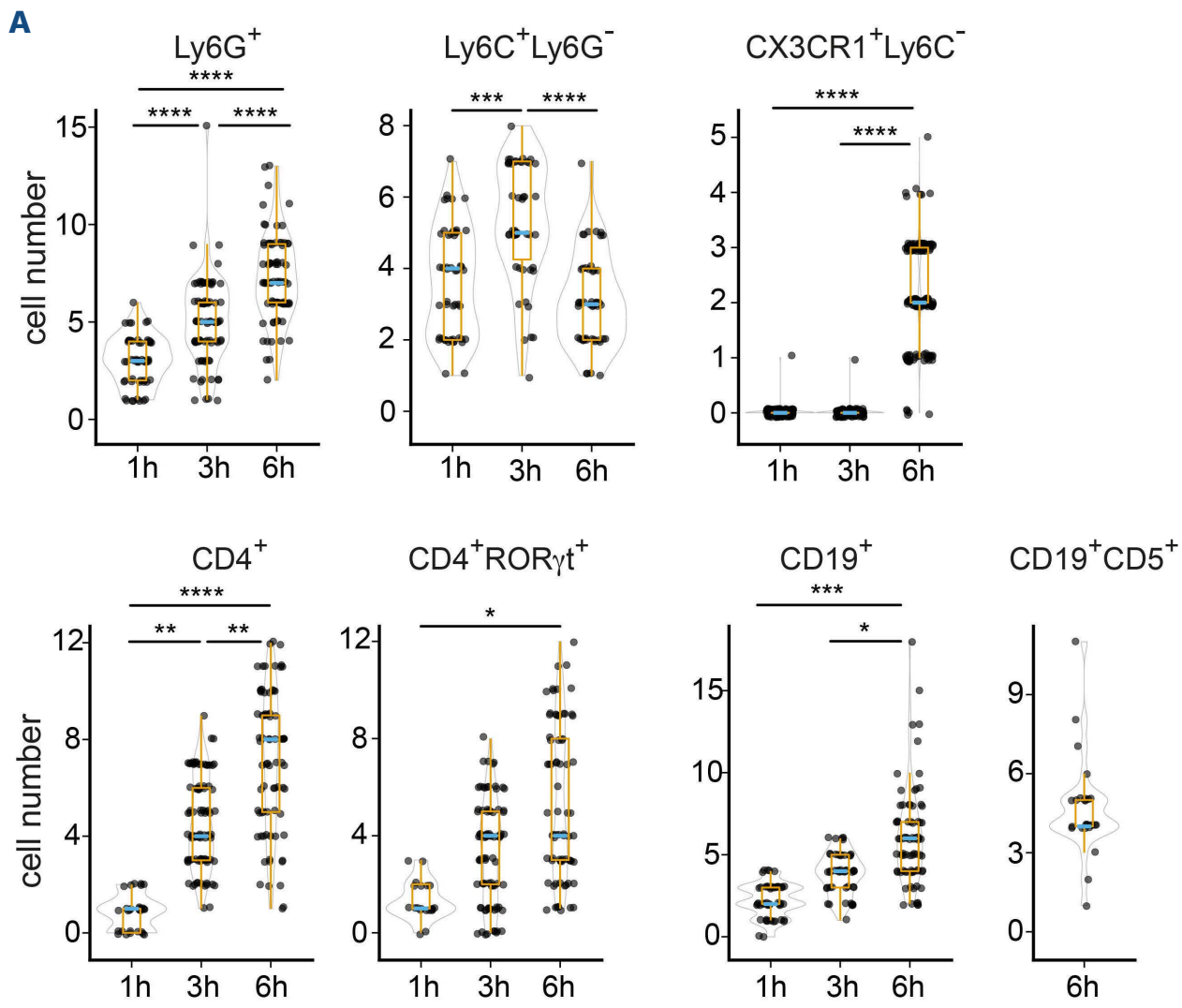

Continued on following page.

Figure 1. Microvascular recruitment of immune cells during systemic infection. (A) Identities and kinetics of arrested immune cells (1-6 hours [h]) in mice infected with *E. coli* (3-6 h) in the liver. (B) Unbiased DAVID cluster analysis of significant altered genes (adjusted *P*<0.05) in uninfected (0 h) and infected (3 h and 18 h) mice. Boxes indicate different mice. Dots refer to different visual fields (A) analyzed from 3-9 animals per group. In violin plots, box plots indicate 25th and 75th percentiles and median is marked by bold lines (A). *P* values were calculated by one-way ANOVA (A). **P*<0.05, ***P*<0.01, ****P*<0.001, *****P*<0.0001.

were adoptively transferred into factor VIIa-supplemented mice (to enhance fibrin levels). Activated T cells decreased fibrin deposition which was prevented by pretreatment of the cells with fibrinolysis inhibitor EACA (*Online Supplementary Figure S2D*). Furthermore, neutralization of uPA *in vivo*, which was preferentially associated with T cells (Figure 2B), enhanced fibrin deposition in control mice, but not in T-helper cell-depleted mice (Figure 4B).

Since CD4$^+$ T cells promoted fibrinolysis during the initial increase in fibrin deposition, we studied the involvement of thrombin-activatable fibrinolysis inhibitor (TAFI) which connects coagulation to fibrinolysis.[17,18] Neutralization of TAFI activity by anti-TAFI antibody that specifically targets activated TAFI did not affect fibrin deposition in control mice consistent with earlier work.[19] Yet, anti-TAFI antibody suppressed fibrin formation in CD4$^+$ T-cell-depleted mice

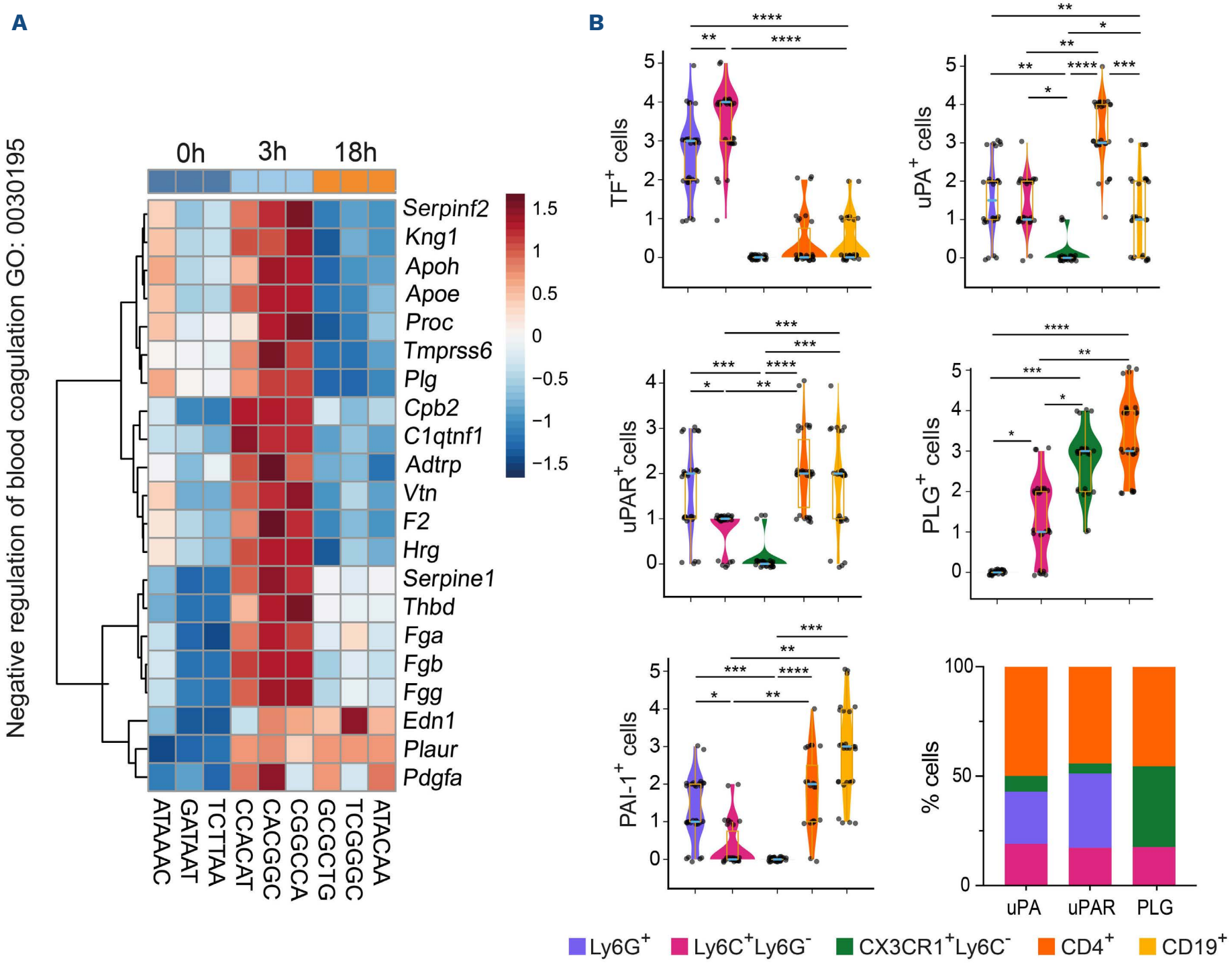

Figure 2. CD4$^+$ T cells express and attract major fibrinolysis regulators. (A) Heatmap showing mRNA expression levels of T-helper cell genes implicated in negative regulation of coagulations of uninfected (0 hours [h]) or infected mice (3 h, 18 h). Boxes indicate different mice. (B) Associations of tissue factor (TF), uPA, uPAR, PLG and PAI-1 with arrested immune cells in mice infected with *E. coli* (3-6 h) in the liver (last graph showing percentage of myeloid cells and CD4$^+$ T cells). Dots refer to different visual fields (B) analyzed from 3-6 animals per group. In violin plots, box plots indicate 25th and 75th percentiles and median is marked by bold lines (B). *P* values were calculated by one-way ANOVA (B). **P*<0.05, ***P*<0.01, ****P*<0.001, *****P*<0.0001.

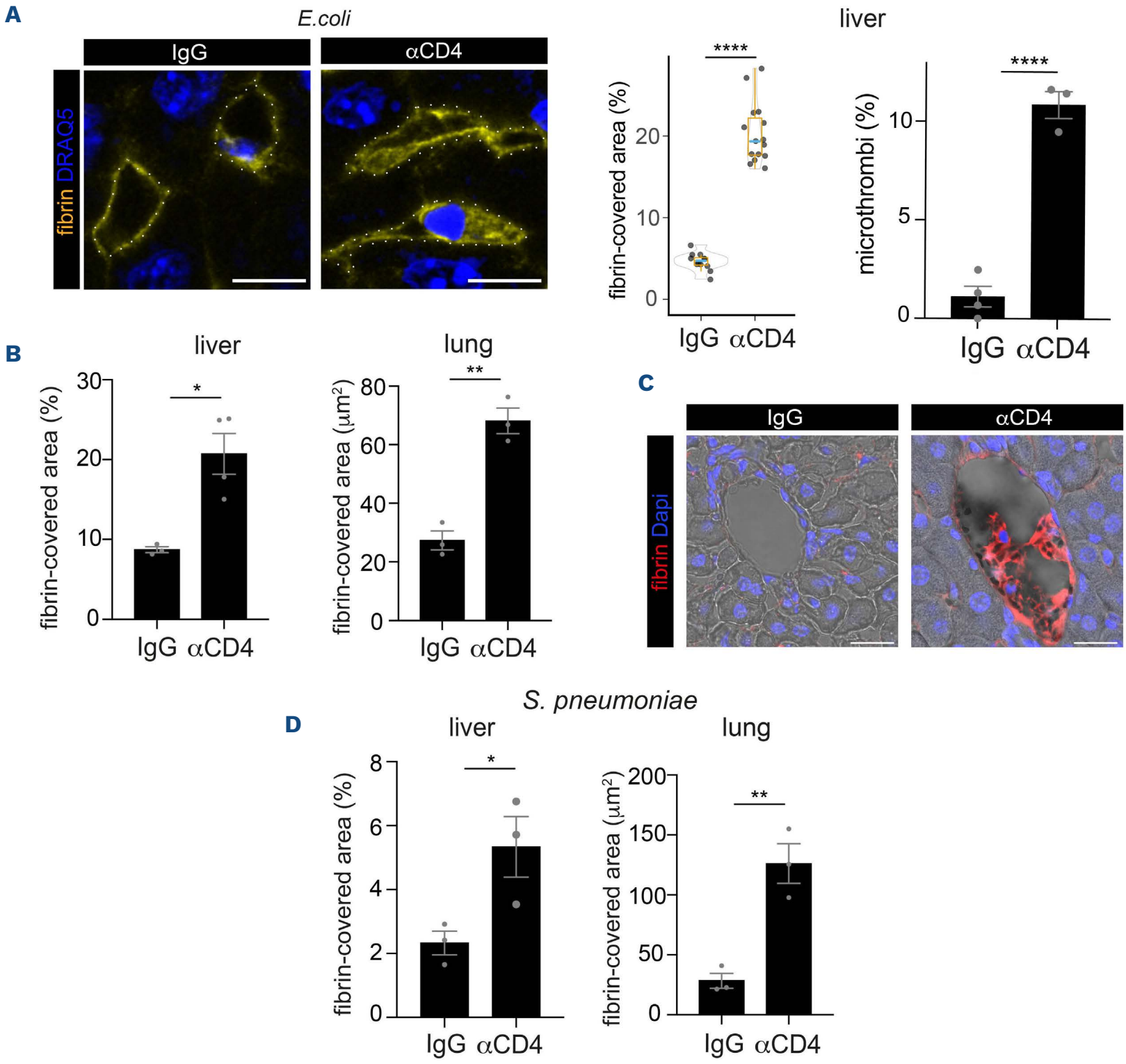

Figure 3. Suppression of intravascular fibrin and microvascular thrombosis by T-helper cells. (A-D) Representative images of liver microcirculation (A, left) and macrovasculature (C) and quantifications of microvascular fibrin deposition and microthrombi in the liver or lung (A, B, D) after infection with *E. coli* (A-C) or after infection with *S. pneumoniae* (D) in T-helper cell-depleted mice (αCD4, 1 hour [h] [A], 3 h [B, C], 6 h [D]). Values indicate intravascular fibrin-covered area as percentage of total intravascular area in the liver (A, B, D) or of intravascular fibrin-covered area per visual field in the lung (B, D). Dotted lines indicate vessel walls. Scale bar, 10 μm (A) or 20 μm (C). Dots refer to different visual fields (A) analyzed from 3 animals per group or the mean of at least 5 visual fields per animal (B, D). In violin plots, box plots indicate 25th and 75th percentiles and median is marked by bold lines (A). *P* values were calculated by unpaired two-tailed *t* test (A, B, D). **P*<0.05, ***P*<0.01, *****P*<0.0001. A_{405}: optical density.

(Figure 4C). Inhibition of TAFI by CPI (also preferentially inhibiting activated TAFI) confirmed that activated TAFI-regulated fibrin deposition in the absence but not in presence of T-helper cells (Figure 4D).

Imaging of the TAFI localization in the microcirculation of control mice indicated a higher association of TAFI with CD4$^+$ T cells compared to other types of leukocytes (Figure 4E). Apart from its cellular association, TAFI was mainly associated with fibrin deposits[20] (Figure 3F, G). Together, this is consistent with regulation of fibrinolysis on both cellular and fibrin surfaces.[21] After CD4$^+$ T-cell depletion, TAFI co-localized almost exclusively with the increased fibrin-covered areas (Figure 4F, G). The extent of TAFI association with fibrin was enhanced in CD4$^+$ T-cell-depleted mice (Figure 4F). Thus, CD4$^+$ T cells prevented fibrinolysis inhibition by TAFI which could be mediated in part by their ability to reduce the association of TAFI with fibrin.

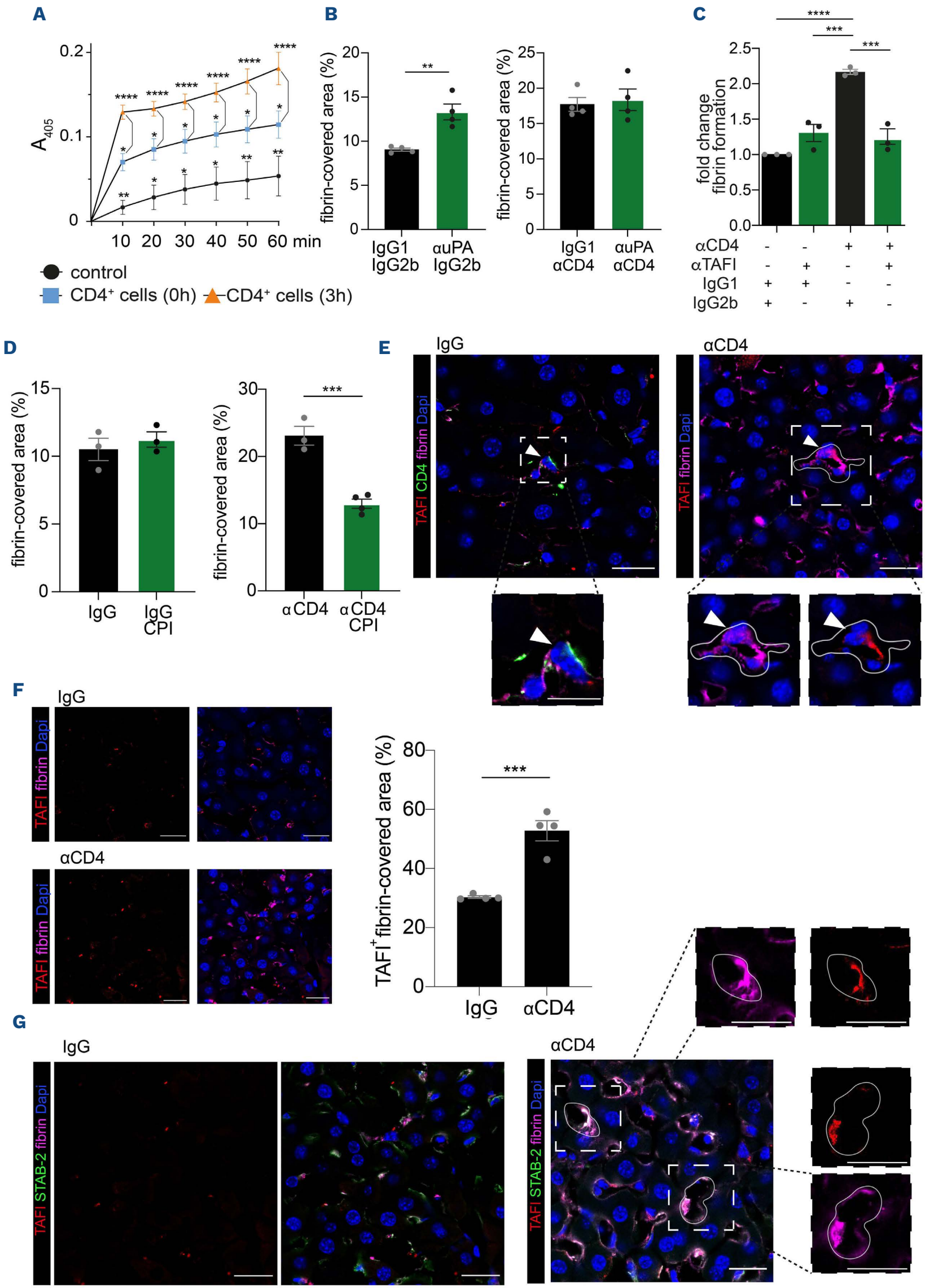

Continued on following page.

Figure 4. Thrombin-activatable fibrinolysis inhibitor increases fibrin deposition in absence of CD4⁺ T cells. (A) Plasmin formation by CD4⁺ T cells from uninfected and infected (3 hours [h]) mice. (B-D) Microvascular fibrin-rich area in liver microcirculation after αCD4 and αUPa treatment (B), thrombin-activatable fibrinolysis inhibitor (TAFI) neutralization (C) or CPI injection (D). (E) Association of TAFI with leukocytes (CD45⁺) and T-helper cells (CD45⁺ CD3⁺) 3 h after infection. (F) TAFI co-localization with CD4⁺ T cells (3 h, immunoglobulin G [IgG]) or other immune cell-rich thrombi (αCD4, 3 h). (G) Association of TAFI with fibrin deposits in vicinity of CD4⁺ T cells (control) or T-cell-free immune cell thrombi (CD4⁺ T-cell depletion). Dots indicate different animals (B-E, G) or mean value from 3 independent samples (A). Data shown as means ± standard error of the mean. *P* values calculated by two-Way ANOVA (A, C) or unpaired two-tailed *t* test (B, D, E, G). *P* values calculated compared to control group (A). **P*<0.05, ***P*<0.01, ****P*<0.001, *****P*<0.0001.

Intravascular fibrin promotes T-cell arrest and activation

Since CD4⁺ T cells partially co-localized with fibrin and components of the coagulation system affect T-cell recruitment,[22] we next investigated whether fibrin contributed to T-cell arrest. In mice deficient for coagulation factor XII (*f12*$^{-/-}$), in which fibrin deposition was inhibited compared to control mice (*Online Supplementary Figure S3A*), arrest of CD4⁺ T cells was strongly reduced compared to WT mice (Figure 5A). In mice treated with rivaroxaban, an inhibitor of coagulation factor Xa that suppressed fibrin formation, arrest of T cells, particularly of Th17 cells, was lowered (*Online Supplementary Figure S3B, C*). Conversely, in plasminogen-deficient mice (*plg*$^{-/-}$) with increased fibrin deposition (from 8.2±0.3% [WT] to 22.8±3.0% fibrin-covered area [*plg*$^{-/-}$]; N=3 mice/group, *P*<0.05), immobilization of CD4⁺ T cells and especially of Th17 cells were augmented (Figure 5B).

T cells recovered at the peak of fibrin formation highly expressed genes involved in T-cell activation (*Online Supplementary Figure S3D*). Notably, CD4⁺ T cells co-localizing with fibrin expressed the activation markers CD69 and CD38 (Figure 5C). Besides their presence in microvessels, activated CD4⁺ T cells were detected in association with thrombi in larger vessels (*Online Supplementary Figure S3E*). Rivaroxaban decreased the levels of arrested CD69⁺ T cells substantially (Figure 5D). Furthermore, T-cell activation was decreased in *f12*$^{-/-}$ mice compared to WT mice (Figure 5E). Rivaroxaban also reduced IFNγ⁺T cells which are another sign of early T-cell activation (Figure 5F).

The high percentages of CD69⁺ T cells in early infection could suggest that T-cell activation may be mediated at least in part by TCR-independent cytokine (or "bystander") activation.[23] In order to check the contribution of TCR-dependent and/or -independent T-cell activation, we prevented TCR-dependent T-cell activation with anti-MHC-II antibody. We also used anti-IL-12p40 antibody to inhibit IL-12- and IL23-mediated T-cell activation thus preventing in particular cytokine-mediated activation of Th17 cells.[24] MHC-II inhibition reduced the amount of activated T cells (Figure 5F). Moreover, anti-IL-12p40 antibody decreased T-cell activation (Figure 5F). Particularly, the levels of activated T cells (CD69⁺ IFNγ⁺) co-localizing with fibrin were decreased by neutralizing MHC-II or IL-12p40 inhibition (*Online Supplementary Figure 3F*). Thus early CD4⁺ T-cell activation by fibrin was supported by TCR- and cytokine-dependent mechanisms.

LFA-1 mediates T-helper cell migration and fibrin-dependent T-cell activation

We next analyzed the source and intravascular movements of the T cells regulating coagulation. In order to investigate their intestinal origin,[25] we photoconverted cells in the small intestine of Kaede mice by UV light to emit red fluorescence instead of green fluorescence (*Online Supplementary Figure S4A*).[26] Twenty-four h later systemic infection was induced with *E. coli*. Photoconverted T-helper cells were detected in the infected livers and to a lesser extent in the lungs (*Online Supplementary Figure S4B*). Most of the intestine-derived T-helper cells in the liver represented Th17 cells.

We used multi-photon intravital microscopy to track the movements of CMTPX-labeled CD4⁺ T cells inside the liver microvasculature. We observed a rapid arrest of part of the circulating T cells while other T cells crawled unidirectionally along the vessel wall or performed alternating movements with and against the blood flow (Figure 6A, B; *Online Supplementary Video S1*). Real-time imaging of T-helper cell movements showed that neutralization of the major T-cell integrin LFA-1[27] with anti-LFA-1 decreased the unidirectional T-cell crawling along the vessel wall (Figure 6C). In contrast, suppression of fibrin formation by rivaroxaban did not alter T-cell migration (*Online Supplementary Figure S5A*; *Online Supplementary Video S2*). Moreover, neutralization of LFA-1 did not change T-cell arrest (Figure 6C). In contrast, it decreased T-cell activation substantially, especially activated T cells that were fibrin-associated (Figure 6D; *Online Supplementary Figure 5B*).

Next, we studied the role of fibrin for T-cell activation in human CD4⁺ T cells *in vitro*. T cells adhering to poly-L- ornithine-coated surfaces where activated via the TCR. The increase in CD69 expression thus observed was unaffected by inhibition of LFA-1 (Figure 6E). Fibrin-coated surfaces noticeably enhanced activation of T cells. T-cell activation by fibrin was largely suppressed by LFA-1 inhibition (Figure 6E). Contrary to the effect of fibrin on T-cell activation, fibrin did not affect migration of human T cells (Figure 6F), agreeing with the *in vivo* observations (*Online Supplementary Figure S4C*). Inhibition of LFA-1 markedly decreased the fibrinolytic activity of the activated T cells (*Online Supplementary Figure S5C*). Thus, LFA-1 mediated both T-cell migration and T-cell activation-dependent fibrinolysis which allowed CD4⁺ T cells most likely to inhibit fibrin deposition both at and distant from sites of T-cell arrest.

Microvascular CD4⁺ T cells and thrombosis in human infections

Pulmonary thrombosis is a deleterious consequence of aberrant immune activation in severe infections including SARS-CoV-2 infection.[28,29] We analyzed autopsies from patients with SARS-CoV-2 infections and compared them with autopsies from patients with influenza virus infections (*Online Supplementary Figure S6A*). CD4⁺ T cells were visualized in different vascular beds of the lung to explore their potential role in thrombosis. The number of CD4⁺ T cells detected in microvessels and larger vessels in patients with SARS-CoV-2 infections was lower compared to patients infected with influenza virus (Figure 7A, B). Thrombotic vessel occlusions were massively increased and pulmonary thrombi tended to be elevated in SARS-CoV-2 infections compared to influenza virus infection (Figure 7C; *Online*

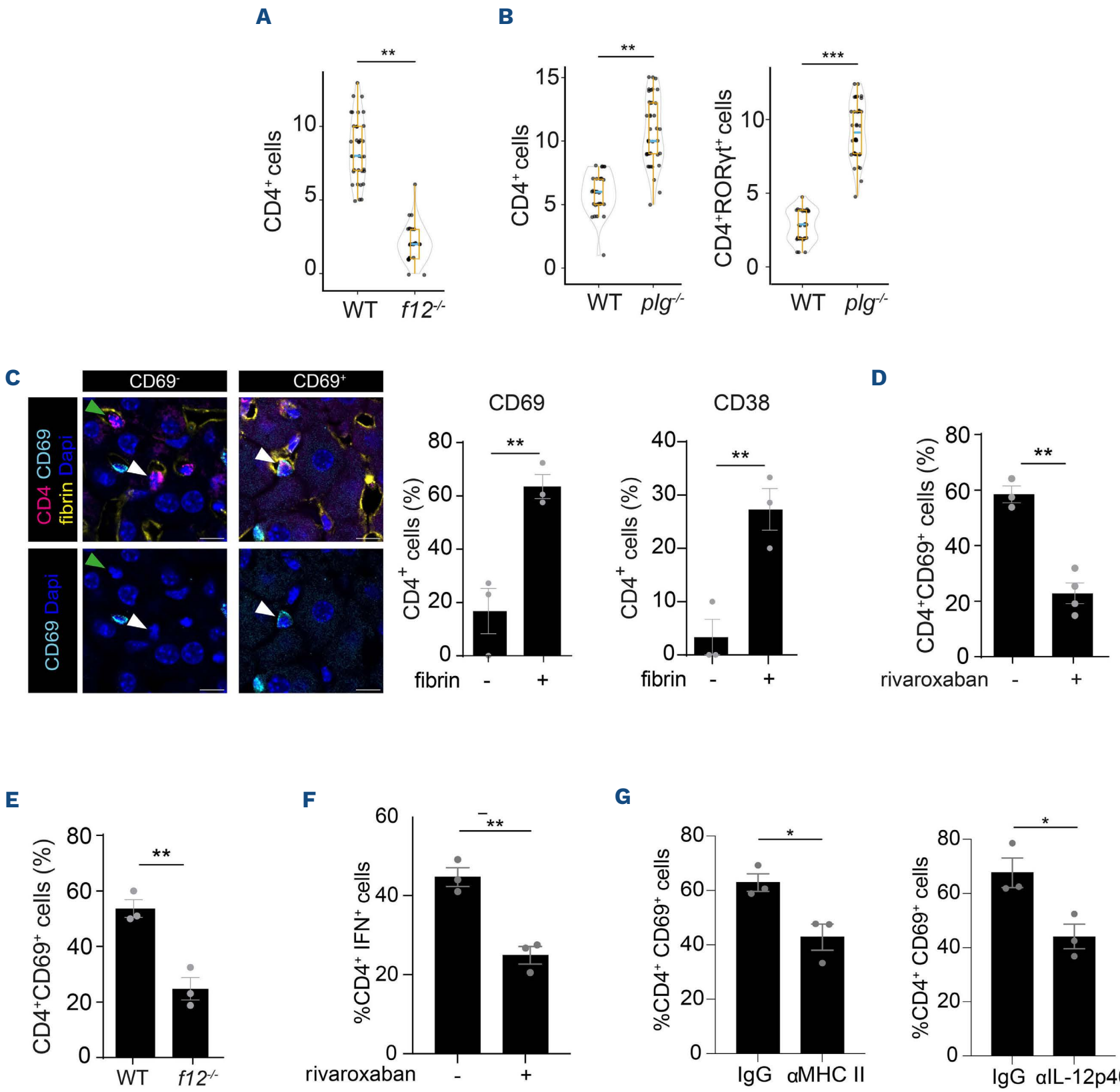

Figure 5. Fibrin critically drives arrest of T-helper cells. (A, B) CD4⁺ T cells or CD4⁺ RORγt⁺ cells (B) arrested in liver microvessels in *f12*$^{-/-}$ mice (6 hours [h]) (A) or *plg*$^{-/-}$ mice (3 h) (B) infected with *E. coli*. (C) Percentage of activated T-helper cells (defined as CD38⁺ or CD69⁺) in fibrin-negative (-) or fibrin-positive (+) areas (3 h). (D, E) T-helper cell activation in the liver microcirculation of rivaroxaban-treated wild-type (WT) mice (D) and *f12*$^{-/-}$ mice (3 h) (E). (F) Percentage of interferon (IFN)γ⁺ T-helper cells in rivaroxaban-treated mice. (G) Percentage of T-helper cell activation in mice treated with αMHC-II or αIL12p40-antibody prior to infection with *E. coli* (3 h). In violin plots, box plots indicate 25th and 75th percentiles and median is marked by bold lines (A, B). A minimum of 3 biological replicates was analyzed (A-G) and dots indicate different animals (C-G). Scale bar, 10 μm (C). Data shown as means ± standard error of the mean. *P* values calculated by unpaired two-tailed *t* test (A-G). **P*<0.05, ***P*<0.01, ***P*<0.01.

Supplementary Figure S6B). TAFI strongly co-localized with fibrin-rich thrombi in SARS-CoV-2 infections (Figure 7D) but barely with intraluminal immune cells. Thus, the enhanced fibrin depositions and TAFI localizations in human infections with strongly reduced microvascular T-cell levels resembled the changes in T-cell-depleted mice. Overall, thrombosis formation in lung vessels during viral infections exhibited an inverse association with microvascular CD4$^+$ T-cell levels (Figure 7E).

Discussion

Innate immune cells including monocytes and neutrophils critically promote intravascular fibrin formation and thereby favor the development of different types of micro- and macrovascular thrombosis.[1-5] They initiate coagulation via the TF-initiated extrinsic pathway of coagulation and propagate fibrin generation by formation of NET. Due to the potentially deleterious consequences of thrombotic vessel occlusions

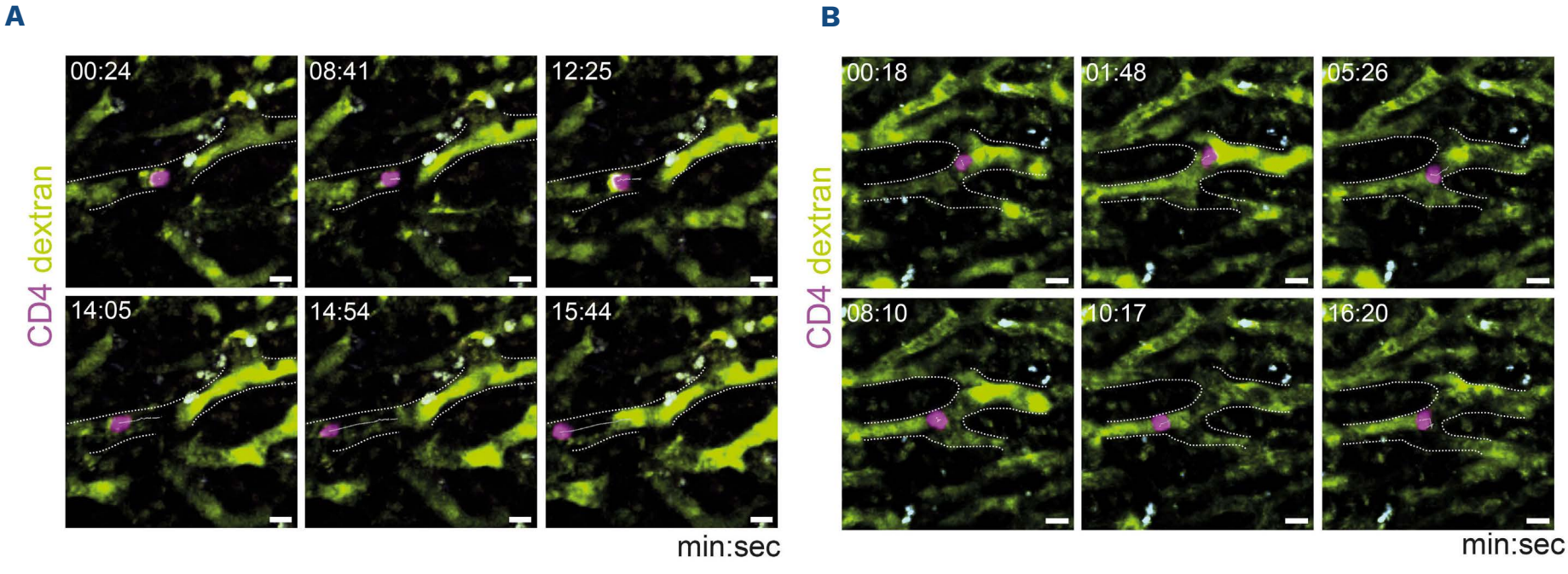

Figure 6. Fibrin activates T-helper cells via LFA-1. (A, B) Time lapse showing intravascular unidirectional (A) and back-forward (B) crawling of CMTPX-labeled CD4$^+$ T cells (magenta) by multi-photon intravital imaging (1-6 hours [h], *E. coli*). Dragon tails visualize the last hundreds of cell movements. Scale bar, 10 μm. (C) Effect of αLFA-1 antibody on unidirectional migration and arrest of T-helper cells in the liver microcirculation analyzed by multi-photon intravital imaging (1-6 h). (D) Percentages of activated CD4$^+$ T cells arrested in microvessels after treatment with αLFA-1 antibody (3 h). (E) Effect of αLFA-1 antibody on activation of isolated human CD4$^+$ T cells *in vitro* on poly-L-ornithine- or fibrin-coated surfaces. (L) Migration of isolated human CD4$^+$ T cells on fibrin- *versus* poly-L-ornithine-coated surfaces. Lines indicate covered distance by single cells. Speed of cell movements is color coded. Dots indicate different animals (D), different videos (C) analyzed in at least 3 animals per group, or isolated cells from different donors (E). Scale bar, 10 μm (A, B) or 20 μm (F). Data shown as means ± standard error of the mean. *P* values calculated by Mann-Whitney test (C), unpaired two-tailed *t* test (D) or two-way ANOVA (E). *P<0.05, **P<0.01.

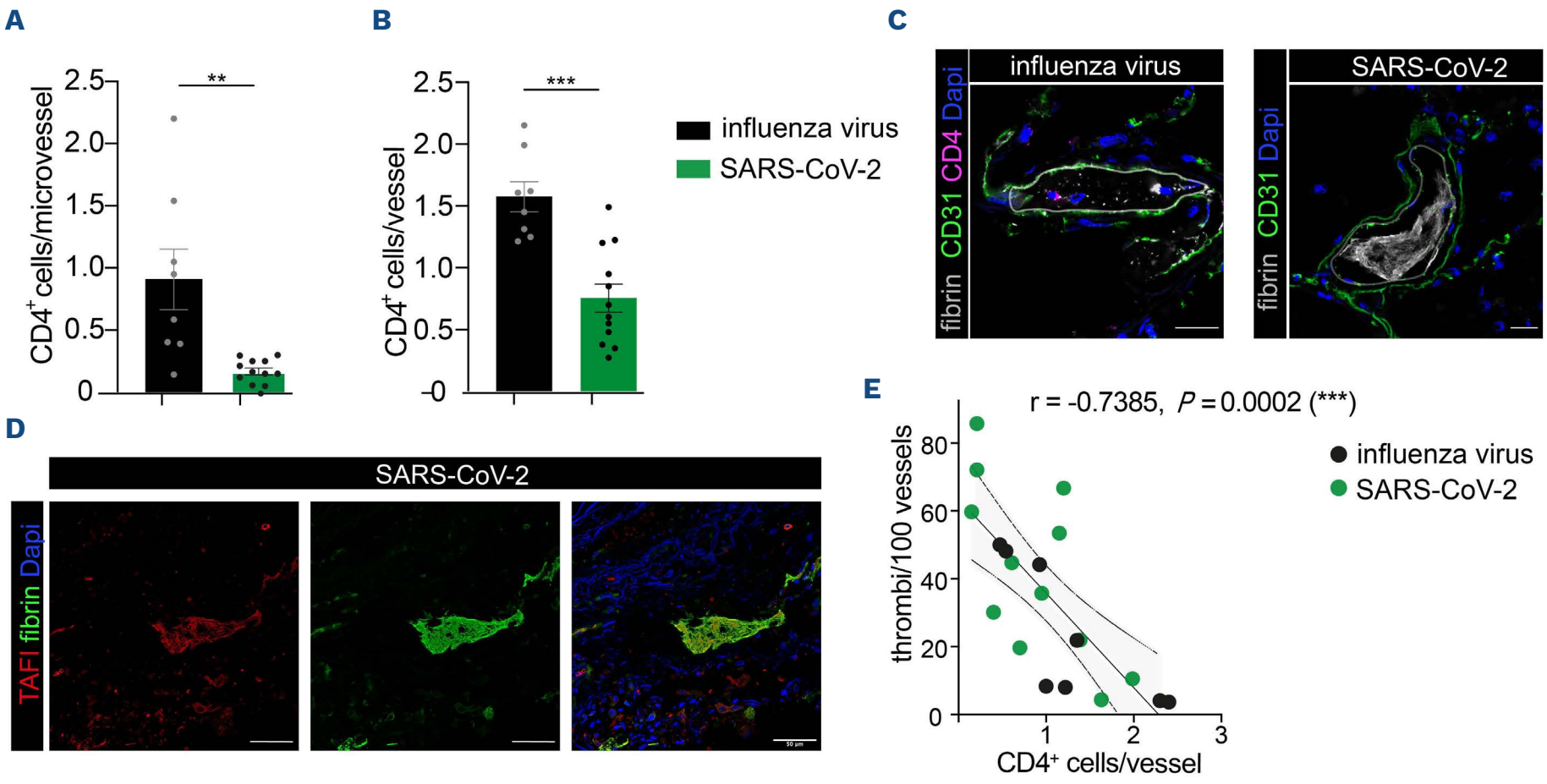

Figure 7. Thrombosis development in human infections is negatively associated with T-cell arrest. (A, B) CD4⁺ T cells in pulmonary vessels with diameter <50 μm (A) or 50-500 μm (B) in patients with SARS-CoV- 2 or influenza virus infections in post-mortem histological analysis of human lung samples with pulmonary infections. (C) Representative image of thrombus in pulmonary vessels of a patients with severe influenza virus (left) or SARS-CoV-2 infection (right). Scale bar, 20 μm. (D) Association of thrombin-activatable fibrinolysis inhibitor (TAFI) with leukocyte-free thrombi during SARS-CoV-2 infection. (E) Correlation between pulmonary thrombosis and intravascular T-helper cells. Scale bar, 20 μm. Dots indicate different patients (A, B, E). Values given as mean ± standard error of the mean. *P* values calculated by unpaired two-tailed *t* test (A, B) or Pearson' correlation with 95% confidence interval (E). ***P*<0.01, ****P*<0.001.

intravascular coagulation needs to be maintained in a homeostatic balance thus disfavoring pathological thrombosis. Although endothelial cells can efficiently protect against excessive intravascular fibrin generation, their anticoagulant and profibrinolytic functions are often compromised during infections, especially at sites of thrombus formation, or they may even be converted into procoagulant mediators.[30] This suggests that additional mechanisms are required to prevent excessive intravascular fibrin and development of thrombosis in infections.

Our study shows that mutual interactions between CD4⁺ T cells and fibrin establish an efficient negative feedback cycle suppressing intravascular fibrin and microvascular thrombosis during infections. Since T-helper cells curtail fibrin deposition during the initial rise in fibrin formation they act as direct antagonists of procoagulant innate myeloid cells, especially counteracting neutrophil dependent fibrin formation. It is well possible that increases in pro-inflammatory cytokines such as IL-1β, TNFα or IL-6 as induced by systemic infection contribute to regulate the inhibitory and enhancing effects of T-helper cells and innate myeloid cells, respectively, on intravascular fibrin deposition.

Intravital imaging and immunohistochemistry analyses reveal that fibrin deposits drive the arrest and LFA-1-dependent activation of CD4⁺ T cells. The arrested T cells mostly represent Th17 cells that are recruited at least in part from the intestine, a major site of residence of Th17 cells. T-helper cell activation appears to require direct fibrin-LFA-1 interactions and is in part mediated by IL-12p40, a component of both IL-12 and IL-23 that preferentially targets Th17 cells,[24] as well as by MHC-II-dependent mechanisms.

Activation and migration of CD4⁺ T cells in turn suppresses fibrin deposition throughout the vasculature by neutralization of TAFI-induced fibrinolysis inhibition and direct stimulation of fibrinolysis. During early infection, CD4⁺ T cells are indeed the major intraluminal carriers of fibrinolysis regulators including plasminogen and their activators. T-helper cell-dependent inhibition of TAFI is shown to be related to the ability of the T cells to prevent the association of TAFI with fibrin, a prerequisite for TAFI-dependent cleavage of C-terminal lysine residues in fibrin[32] and subsequent fibrinolysis inhibition. This mechanism could contribute to explain why (at presumably normal T-cell levels) TAFI deficiency does not result in substantial changes in fibrin formation and thrombosis development.[19]

Dysregulations of coagulation are characteristics of severe SARS-CoV-2 infections and might sustain in part long-term

sequelae of Covid-19 infections.[33-35] Since activated CD4$^+$ T cells promote fibrinolysis and their loss increases intravascular fibrin via TAFI, the inverse relations between T-cell arrest and thrombosis observed here suggest that also in human infections CD4$^+$ T cells might protect from pathological thrombosis. Consequently, lymphopenic conditions, a common feature of fatal infections and other diseases,[36-38] critically dysregulate thrombosis *per se*. The opposing effects of neutrophils *versus* CD4$^+$ T cells, the major circulating lymphocyte fraction in human blood, suggest why increased neutrophil/lymphocyte ratios (for example[39]) predispose for different types of pathological thrombosis.

Disclosures

No conflicts of interest to disclose.

Contributions

TTM, MP, MT, TL, JKLH, SMe, RB, FK, LGP, RÖ, TE, JL, MV, HY, HI-A performed experiments and evaluated data. TTM, HI-A, and BE analyzed data. CW, AZK, KTP, SH, SM contributed to interpretation and presentation of data. CS, HI-A, BE coordinated and supervised the study. CT, MWy, HR, SE, PvH, CS, DT, RR, SH, MM, SM, DT, UK provided resources. BE and SM secured funding. BE conceived the study and wrote the manuscript with the help of all other authors.

Acknowledgments

We are grateful to Susanne Pfeiler, Pia Vornewald, Dominic van den Heuvel, Daniel Setzensack, Meike Miller, Anna Titova, Arwa Obaid, Wolfgang Wilfert, Lusine Saroyan and Anastasios Giannou for their contributions at different stages of the study. We would like to kindly thank the Bioimaging Core Facility of the Biomedical Center of LMU Munich, especially Steffen Dietzel, for advice and help. We are grateful to Paul Declerck, Michael Ploug and Thomas Bugge for their helpful advice as well as for providing antibodies. We thank the German Center for Lung Research (DZL) for providing tissue sections from autopsies.

Funding

The study was supported by grants from the Deutsche Forschungsgemeinschaft SFB1321 (to BE and SM), SFB1123 (to SM and BE) and SFB 914 (to HI-A, SM and CS).

Data-sharing statement

Please direct all requests for materials and correspondence to the corresponding authors.

References

1. Iba T, Levy JH. Inflammation and thrombosis: roles of neutrophils, platelets and endothelial cells and their interactions in thrombus formation during sepsis. J Thromb Haemost. 2018;16(2):231-241.
2. Van Bruggen S, Martinod K. The coming of age of neutrophil extracellular traps in thrombosis: where are we now and where are we headed? Immunol Rev. 2023;314(1):376-398.
3. Wu C, Lu W, Zhang Y, et al. Inflammasome activation triggers blood clotting and host death through pyroptosis. Immunity. 2019;50(6):1401-1411.
4. Engelmann B, Massberg S. Thrombosis as an intravascular effector of innate immunity. Nat Rev Immunol. 2013;13(1):34-45.
5. Opal SM, Esmon CT. Bench-to-bedside review: functional relationships between coagulation and the innate immune response and their respective roles in the pathogenesis of sepsis. Crit Care. 2002;7(1):23-38.
6. Bonaventura A, Vecchié A, Dagna L, et al. Endothelial dysfunction and immunothrombosis as key pathogenic mechanisms in COVID-19. Nat Rev Immunol. 2021;21(5):319-329.
7. van der Poll T, van de Veerdonk FL, Scicluna BP, Netea MG. The immunopathology of sepsis and potential therapeutic targets. Nat Rev Immunol. 2017;17(7):407-420.
8. Tomura M, Yoshida N, Tanaka J, et al. Monitoring cellular movement in vivo with photoconvertible fluorescence protein "Kaede" transgenic mice. Proc Natl Acad Sci USA. 2008;105(31):10871-10876.
9. Lechner, M., Engleitner, T., Babushku, T. et al. Notch2-mediated plasticity between marginal zone and follicular B cells. Nat Commun. 2021;12(1):1111.
10. Kedl RM, White JT. Foreign antigen-independent memory-phenotype CD4+ T cells: a new player in innate immunity? Nat Rev Immunol. 2018;18(3):1.
11. Skendros P, Mitsios A, Chrysanthopoulou A, et al. Complement and tissue factor–enriched neutrophil extracellular traps are key drivers in COVID-19 immunothrombosis. J Clin Invest. 2020;130(11):6151-6157.
12. Schechter ME, Andrade BB, He T, et al. Inflammatory monocytes expressing tissue factor drive SIV and HIV coagulopathy. Sci Transl Med. 2017;9(405):eaam5441.
13. Antoniak S, Mackman N. Multiple roles of the coagulation protease cascade during virus infection. Blood. 2014;123(17):2605-2613.
14. Shahneh F, Grill A, Klein M, et al. Specialized regulatory T cells control venous blood clot resolution through SPARC. Blood. 2021;137(11):1517-1526.
15. Nicklas JM, Gordon AE, Henke PK. Resolution of deep venous thrombosis: proposed immune paradigms. Int J Mol Sci. 2020;21(6):2080.
16. Loef EJ, Sheppard HM, Birch NP, Dunbar PR. Plasminogen and plasmin can bind to human T cells and generate truncated CCL21 that increases dendritic cell chemotactic responses. J Biol Chem. 2022;298(7):102112.
17. Sillen M, Declerck PJ. Thrombin activatable fibrinolysis inhibitor (TAFI): an updated narrative review. Int J Mol Sci. 2021;22(7):3670.
18. Nesheim M, Wang W, Boffa M, Nagashima M, Morser J, Bajzar L. Thrombin, thrombomodulin and TAFI in the molecular link between coagulation and fibrinolysis. Thromb Haemost. 1997;78(01):386-391.
19. Nagashima M, Yin Z-F, Zhao L, et al. Thrombin-activatable fibrinolysis inhibitor (TAFI) deficiency is compatible with murine

life. J Clin Invest. 2002;109(1):101-110.
20. Satoh T, Satoh K, Yaoita N, et al. Activated TAFI promotes the development of chronic thromboembolic pulmonary hypertension: a possible novel therapeutic target. Circ Res. 2017;120(8):1246-1262.
21. Chapin JC, Hajjar KA. Fibrinolysis and the control of blood coagulation. Blood Rev. 2015;29(1):17-24.
22. Ryu JK, Petersen MA, Murray SG, et al. Blood coagulation protein fibrinogen promotes autoimmunity and demyelination via chemokine release and antigen presentation. Nat Commun. 2015;6(1):8164.
23. Lee H, Jeong S, Shin E-C. Significance of bystander T cell activation in microbial infection. Nat Immunol. 2022;23(1):13-22.
24. Mills KHG. IL-17 and IL-17-producing cells in protection versus pathology. Nat Rev Immunol. 2023;23(1):38-54.
25. Stockinger B, Omenetti S. The dichotomous nature of T helper 17 cells. Nat Rev Immunol. 2017;17(9):535-544.
26. Krebs CF, Reimers D, Zhao Y, et al. Pathogen-induced tissue-resident memory T H 17 (T RM 17) cells amplify autoimmune kidney disease. Sci Immunol. 2020;5(50):eaba4163.
27. Walling BL, Kim M. LFA-1 in T Cell Migration and differentiation. Front Immunol 2018;9:952.
28. Ackermann M, Verleden SE, Kuehnel M, et al. Pulmonary vascular endothelialitis, thrombosis, and angiogenesis in Covid-19. N Engl J Med. 2020;383(2):120-128.
29. Afzali B, Noris M, Lambrecht BN, Kemper C. The state of complement in COVID-19. Nat Rev Immunol. 2022;22(2):77-84.
30. Yau JW, Teoh H, Verma S. Endothelial cell control of thrombosis. BMC Cardiovasc Disord. 2015;15:130.
31. Cooper AM, Khader SA. IL-12p40: an inherently agonistic cytokine. Trends Immunol. 2007;28(1):33-38.
32. Wang W, Boffa MB, Bajzar L, Walker JB, Nesheim ME. A study of the mechanism of inhibition of fibrinolysis by activated thrombin-activable fibrinolysis inhibitor. J Biol Chem. 1998;273(42):27176-27181.
33. Morrow AJ, Sykes R, McIntosh A, et al. A multisystem, cardio-renal investigation of post-COVID-19 illness. Nat Med. 2022;28(6):1303-1313.
34. Couzin-Frankel J. Clues to long COVID. Science. 2022;376(6599):1261-1265.
35. Al-Aly Z, Bowe B, Xie Y. Long COVID after breakthrough SARS-CoV-2 infection. Nat Med. 2022;28(7):1461-1467.
36. Moss P. The T cell immune response against SARS-CoV-2. Nat Immunol. 2022;23(2):186-193.
37. Drewry AM, Samra N, Skrupky LP, Fuller BM, Compton SM, Hotchkiss RS. Persistent lymphopenia after diagnosis of sepsis predicts mortality. Shock. 2014;42(5):383-391.
38. Zidar DA, Al-Kindi SG, Liu Y, et al. Association of lymphopenia with risk of mortality among adults in the US general population. JAMA Netw Open. 2019;2(12):e1916526.
39. Hu J, Cai Z, Zhou Y. The association of neutrophil-lymphocyte ratio with venous thromboembolism: a systematic review and meta-analysis. Clin Appl Thromb Hemost. 2022;28:10760296221130061.